RESISTIVITY ANOMALIES AND SUPERCONDUCTIVITY IN NbS_3

Mitsuru Izumi, Toshiki Nakayama, Ryozo Yoshizaki[+],
Kunimitsu Uchinokura, Toshiaki Iwazumi, Taisaku Seino,
and Etsuyuki Matsuura

Institute of Physics, University of Tsukuba
Sakura-mura, Ibaraki 305, Japan
[+]Institute of Applied Physics, University of Tsukuba
Sakura-mura, Ibaraki 305, Japan

ABSTRACT - The dc and ac electrical conductivity measurements are reported on a quasi-one-dimensional conductor NbS_3. Sulfur-rich NbS_3 shows semiconducting property. Crystals are divided into two groups. One exhibits a resistivity anomaly around 140 K, and the other shows two successive resistivity anomalies around 235 and 140 K. Metallic NbS_3 was obtained by annealing the sulfur-rich or nearly stoichiometric crystals in a vacuum. In metallic NbS_3, existence of a superconducting phase transition below 2.15 K was observed on the basis of resistance and critical magnetic field measurements.

INTRODUCTION

Transition-metal trichalcogenides show various electrical transport properties [1]. NbS_3 has been classified as a diamagnetic semiconductor. Rijnsdorp and Jellinek [2] have found that NbS_3 is triclinic and belongs to the space group $P\bar{1}$ with $a=4.963$ Å; $b=6.730$ Å; $c=9.144$ Å; $\alpha=90^\circ$; $\beta=97.17^\circ$ and $\gamma=90^\circ$. The crystal structure is composed of quasi-one dimensional NbS_3 chains and each chain includes distorted Nb-Nb pairs along the b axis which has been interpreted as a formation of the charge-density wave (CDW) with the modulation period $2b_0$, where b_0 is defined as an interatomic distance of niobium along the chain axis in undistorted phase of NbS_3 (hypothetical). Structure of the undistorted phase of NbS_3 is expected to be similar to that of ZrS_3 determined by Furuseth et al. [3]. Schematic view of the

locations of Nb atoms in one NbS_3 chain is shown in Fig. 1. Grigoryan and Novoselova [4] have observed that temperature dependence of the electrical conductivity of NbS_3 shows semiconducting property.

Within the last half decade the existence of several polytypic phases of NbS_3 has been reported. Cornelissens et al. [5] and later Boswell and Prodan [6] observed by electron microscopy that the second phase of NbS_3(type II) shows the existence of the superlattice spot with the incommensurate period of less than $3b_{\emptyset}^{*}$ ($\sim 2.9b_{\emptyset}$). After Cornelissens et al. we denote the semiconducting NbS_3 determined by Rijnsdorp and Jellinek as the type I NbS_3. Recently, Roucau et al. [7] reexamined the type II crystals by electron diffraction. At room temperature two distortion wave vectors, ($\emptyset.5a^{*}$, $\emptyset.297b_{\emptyset}^{*}$, $\emptyset$) and ($\emptyset.5a^{*}$, $\emptyset.353b_{\emptyset}^{*}$, $\emptyset$) were observed. They also indicated that monoclinic parameters are a=9.9 Å; b=3.4 Å($=b_{\emptyset}$); c=18.3 Å and $\beta=97^{\circ}$.

Zettl et al. [8] have synthesized another phase of NbS_3 (type III). According to their x-ray study, the lattice constants along the a and c axes resemble those of type I NbS_3. The monoclinic angle β was 98-99°.

In this paper, we will report firstly the results of dc and ac electrical conductivity measurements of semiconducting NbS_3. The sample which has good stoichiometry behaves as a highly-gapped semiconductor, while sulfur-rich NbS_3 shows resistivity anomaly. Secondly we will establish the existence of a metallic NbS_3 and will report its superconducting phase transition below 2.15 K on the basis of resistance and critical magnetic field measurements.

SAMPLE PREPARATION

To obtain good quality of a single crystal of NbS_3, we used 99.99 at.% niobium powder for optics standard by SPEX. The certificate of analysis shows that the content of Ta is less than 100 ppm. We also used 99.999 at.% sulfur chunk. A quartz ampoule which contains niobium and sulfur was evacuated and sealed. The amounts of the metal and chalcogen are non-stoichiometric and excess sulfur acts as a mineralizing agent to encourage homogeneity. Sulfur-rich crystal was obtained by direct reaction of the elements in temperature profile of 700° C to 600° C, and also could be

found in temperature profile of 600°C to 500°C. Nearly stoichiometric NbS_3 was obtained mostly in the temperature profile of 600°C to 500°C. Metallic crystal was obtained by annealing the sulfur-rich or nearly stoichiometric crystal between 600°C and 650°C in a vacuum. After annealing, single crystals of sulfur were found together with the metallic crystals of NbS_x in the ampoule. As will be shown in the following, the resistivity at room temperature, the value of $x \sim 3$ of NbS_x and superconducting transition temperature T_c for the metallic NbS_x depend on the batch. More systematic study (e.g. sulfur-pressure dependence in the quartz ampoule) of the crystal synthesis is absolutely necessary to clarify the mechanism of an interpolytypic phase transition and/or evaporation of sulfur. Crystals were analyzed quantitatively for only Nb content by an inductively-coupled-plasma-optical-emission spectrometer for every batch. The amount of sulfur was estimated under the assumption that the remaining weight comes from sulfur. The results for the sulfur-rich crystals showed that the composition was $NbS_{3.5-4.0}$. X-ray data of the sulfur-rich crystal by a four-circle diffractometer and previous x-ray data of type I NbS_3 were essentially the same. We consider, therefore, that the crystal structures of the sulfur-rich crystals and type I crystal are the same. We denote the sulfur-rich crystals as the sulfur-rich NbS_3. On the other hand, we denote the metallic crystals ($NbS_{2.5-3.4}$ by chemical analysis) as the metallic NbS_3 in the following. Characteristics of the typical samples are shown in Table I.

EXPERIMENTAL TECHNIQUES

Measurements of the dc electrical resistivity were made by the conventional four-probe method. The electrical contacts were obtained by silver paste (DuPont 4929). Dc current flow was supplied along the chain b axis. Ac conductance measurement was performed by the use of an impedance analyzer (YHP model 4192A). In this case, two-probe method was used. The maximum ac voltage was 1.1 V. Typical length of the sample was 700-800 μm.

For the observation of the superconducting transition in metallic NbS_3, the low current density (0.3-2.2 A/cm^2, which is much smaller than the typical critical current, 100 A/cm^2)

was used. The samples were placed in a ^3He cryostat with a superconducting solenoid magnet. Below 3.2 K the sample was preserved in the liquid ^3He.

RESULTS AND DISCUSSION

(1) X-ray diffraction analysis of various phases of NbS_3

X-ray oscillation photograph presents the intriguing structural variation along the b axis of NbS_x with x~3. A conventional Weissenberg camera was used in the present study. As an x-ray source, MoKα radiation was employed. The crystal data of the sample #2 or 3 (Note that we did not confirm the electrical transport property of the sample provided for x-ray study and the type A NbS_3 (#2) and the type B NbS_3 (#3) were obtained from the same batch), and #5 at room temperature are the same as those of type I crystal.

Figure 2 shows a typical set of the b-axis oscillation photographs of NbS_x. Figures 2(a)-2(d) correspond to the photographs of the sample #2 or 3 (sulfur-rich NbS_3), #4, #5, and #6, in this order. It is clear that there are two different types in length of the b* axis. In one type of the crystals the length of the b* axis is similar to that of type I crystal (Figs. 2(a), 2(b) and 2(c)), i.e., $b^*=\emptyset.5b^*_\emptyset$. In the other type, $b^*=b^*_\emptyset$ (Fig. 2(d)). For the former type of samples, Figs. 2(a) and 2(c) show that the reflectional intensity of 2n+1 (n:integer) layer-lines is not much weaker than that of 2n layer-lines, and Fig. 2(b) shows that 2n+1 layer-lines have very weak one. In the latter type (i.e. Fig. 2(d)), the layer-lines corresponding to the 2n+1 in the former type were not observed. Observation of weak 2n+1 layer-lines in the b-axis oscillation photograph implies the existence of a modulation period of $2b_\emptyset$. The crystal data other than b* axis of the sample #4 and #6 were not determined in the present study because well-formed single crystals were not obtained and it was quite difficult to make the crystals into powder. The detailed crystal data for these compounds would eventually clarify the origin of the metallic NbS_3. The point is whether the metallic NbS_3 originates from an interpolytypic phase transition or not.

(2) Resistivity anomalies in sulfur-rich phase of NbS_3

As shown in Table I, the crystals of sulfur-rich NbS_3 are divided into two groups. One is the sulfur-rich NbS_3 which exhibits a resistivity anomaly in the vicinity of 140 K (we denote this crystal as type A NbS_3) and the other is the sulfur-rich NbS_3 which shows two successive resistivity anomalies in the vicinity of 235 and 140 K (we denote this crystal as type B NbS_3). Figure 3 shows the temperature dependences of the dc resistivity of nearly stoichiometric NbS_3 and three samples of the type A NbS_3. Resistivity (ρ) of the nearly stoichiometric NbS_3 obeys the formula, $\rho = \rho_0 \exp(\Delta/2kT)$. It gives the band-gap energy Δ of 0.66 eV below room temperature and does not show anomaly down to 120 K. The band-gap energy is in good agreement with that reported on NbS_3 by Grigoryan and Novoselova (0.72 eV) [see Fig. 3 of ref. 4]. In the type A NbS_3 the typical value of the resistivity at room temperature was 40-50 ohm-cm. Between 130 and 82 K the resistivity is described as $\rho = \rho_0 \exp(E/k_BT)$ with E=90 meV. Figures 4(a) and 4(b) show the temperature dependence of the conductivity and its derivative with respect to temperature at several frequencies between 10 Hz and 13 MHz. The singularity of the conductivity is clearly seen in the derivative around 140 K and it is more pronounced with increasing frequency. This resistivity anomaly is similar to that observed by Zettl et al. [8] for the type III NbS_3. The derivative of the conductivity, however, has a broad peak even for dc measurement in the type III NbS_3. The activation energy reported by Zettl et al. is 152 meV, which is much larger than that of type A NbS_3.

Figure 5(a) shows the temperature dependence of the conductivity of typical sample of type B NbS_3 at several frequencies between 10 Hz and 13 MHz. The conductivity was normalized at 280 K. Two successive resistivity anomalies were observed around 235 and 140 K [9]. The derivative of the conductivity with respect to temperature is shown in Fig. 5(b). The singularity around 140 K is more pronounced with increasing frequency, while the pattern of the singularity at about 235 K does not depend on frequency.

(3) Superconducting phase transition in metallic NbS_3

Temperature dependence of the dc electrical resistance for the metallic NbS_3 was measured from 280 to 0.3 K. Measurement of the superconductivity of the metallic NbS_3 was concentrated on the samples of the batch #5. In the following, the sample #5 means that the sample belongs to the batch #5. The resistivity was $1\text{-}3\times10^{-3}$ ohm-cm at 4.2 K and the residual resistance ratio, R.R.R. ($R_{280\ K}/R_{4.2\ K}$) was 1.9-2.1 for all of the batches that we have already studied. Magnetic field dependence of the resistivity was measured at 4.2 K to survey the quantum oscillations. The direction of the magnetic field (B) was perpendicular to both the a-b plane and the current flow. Transverse magnetoresistance was very weak up to 80 kG. The resistance increases by less than 1 % of the zero magnetic field resistance.

Figure 6 exhibits the resistivity of the sample #5 of metallic NbS_3 in zero magnetic field as a function of temperature between 4.54 and 0.3 K. Abrupt decrease of the resistivity was observed. The resistivity ratio ($R_{4.54\ K}/R_{0.3\ K}$) was $\sim$10000. Resistive transition curves as a function of magnetic field are shown in Fig. 7 for the sample #5 under the $B \perp$ a-b plane configuration. With decreasing temperature the transition curve shifts toward higher magnetic field. From these facts we assert that the metallic NbS_3 undergoes superconducting transition. We define the transition temperature T_c as the temperature at the midpoint in the resistive transition curve. T_c of the sample #5 in a zero magnetic field was 1.65 K. There is little influence on T_c of the fragile nature during cooling to T_c. We cooled down the same sample from room temperature to 0.3 K for three times, but T_c did not change within the experimental errors. The existence of high critical magnetic field indicates that the superconductivity is classified as type II.

The values of T_c's of several samples in the different batches are listed in Table I. The transition temperature are slightly dependent on samples in the same batch. The variation of T_c was less than $\pm$ 0.1 K in the same batch. Larger variation of T_c exists among the samples which were obtained in the different batches. All of the measured samples of metallic NbS_3 showed superconducting transitions. The highest T_c was 2.15 K

of the sample #6. The sample #6 does not show $0.5b^*_0$ periodicity (see Fig. 2) and the samples #4 (T_c=1.45 K) and #5 (T_c= 1.65 K) show $0.5b^*_0$ periodicity. On the basis of the crystal structure only along the b axis at room temperature, we consider that there exist two types of samples. Evaporation of sulfur atoms and/or interpolytypic phase transition may be the origin of this complicated situation. The observation of the structure of $0.5b^*_0$ at room temperature and the metallic property including the superconducting transition of the samples #4 and #5 may lead to the coexistence of the CDW and superconductivity at low temperature.

Figure 8 shows the temperature dependence of the second critical magnetic field ($H_{c2\perp}$) as a function of T/T_c in the B$\perp$ a-b plane configuration. $H_{c2\perp}$ was taken as the magnetic field at the midpoint in the resistive transition curve. It was found that $H_{c2\perp}$ decreases near T_c with a positive curvature as the temperature increases. Similar curvature has been observed in $(SN)_x$ [10]. We roughly estimate $H_{c2\perp}$ (T=0 K) to be 20-23 kG by extrapolation to T/T_c=0.

We also measured $H_{c2//}$ in the B//b-axis configuration at limited points of T/T_c. Anisotropy of the critical field $t(=H_{c2//}/H_{c2\perp})$ is plotted in Fig. 9. The value of t depends on temperature and increases with increasing temperature. Similar result has been obtained on $(SN)_x$ and the effect of the fiber size on the critical field has been discussed [10,11]. The magnitude of the temperature-dependent anisotropy (t) was explained by the intrinsic anisotropy of the electronic band structure and the anisotropy caused by tunneling between chains, both of which frequently lead to the highly anisotropic coherence length in low-dimensional materials. The qualitative resemblance of the superconducting characteristics of $(SN)_x$ and the metallic NbS_3 suggests that we cannot neglect the fibrous morphology of the crystal for the analysis of superconducting property of the metallic NbS_3.

CONCLUSION

Quasi-one-dimensional conductor NbS_3 shows various electrical properties. Nearly stoichiometric NbS_3 behaves as a highly-

gapped semiconductor with the band-gap energy of Ø.66 eV. Two types of sulfur-rich NbS_3 were synthesized. One shows the resistivity anomaly around 14Ø K and its electrical conduction obeys the activation law with the energy of ~9Ø meV between 13Ø and 82 K. The other exhibits two successive resistivity anomalies around 235 and 14Ø K. Metallic NbS_3 was obtained by annealing the sulfur-rich or nearly stoichiometric crystals of NbS_3 in a vacuum. Existence of a superconducting state was found out on the basis of resistance and critical magnetic field measurements. X-ray analysis confirmed that the sample of metallic NbS_3 which has high superconducting transition temperature has no Peierls distorted structure along the chain b* axis.

ACKNOWLEDGEMENTS

The authors are grateful to Dr. K. Notsu of the Chemical Analysis Center of University of Tsukuba for the analysis of the crystals by an inductively-coupled-plasma-optical-emission spectrometer. They also appreciate the collaboration of T. Okamura, K. Fukuhara, K. Yuhara and S. Harada in the early stage of the investigation.

REFERENCES

[1] T. Sambongi, M. Ido, K. Tsutsumi, M. Yamamoto, T. Takoshima, and Y. Abe, Quasi-One-Dimensional Conductors I, ed. by S. Barisic, A. Bjelis, J. R. Cooper, and B. Leontic (Springer, Berlin, 1979) Vol. 95 of Lecture Notes in Physics, p. 349.

[2] J. Rijnsdorp and F. Jellinek, J. Solid State Chem. 25, 325 (1978).

[3] S. Furuseth, L. Brattas, and A. Kjekshus, Acta Chem. Scand. A29, 623 (1975).

[4] L. A. Grigoryan and A. V. Novoselova, Dokl. Akad. Nauk CCCP 144, 795 (1962).

[5] T. Cornelissens, G. Van Tendeloo, J. Landuyt, and S. Amelinckx, phys. stat. sol. (a) 48, K5 (1978).

[6] F. W. Boswell and A. Prodan, Physica 99B, 361 (1980).

[7] C. Roucau, T. Granier, and R. Ayroles, J. de Physique (in press).

[8] A. Zettl, C. M. Jackson, A. Janossy, G. Grüner, A. Jacobson, and A. H. Thompson, Solid State Commun. 43, 345 (1982).

[9] Recently Shimono et al. (Keio University, Japan) also found the existence of NbS_3 which shows two-seccessive resistivity anomalies around 240 and 140 K (private communication).

[10] L. J. Azevedo, W. G. Clark, G. Deutscher, R. L. Greene, G. B. Street, and L. J. Suter, Solid State Commun. 19, 197 (1976).

[11] J. F. Kwak, R. L. Greene, and W. W. Fuller, Phys. Rev. B20, 2658 (1979).

Table I. Characteristics of NbS_3 samples

batch/sample	stoichiometric NbS_3	sulfur-rich NbS_3		metallic NbS_3		
	#1 (type I)	#2(type A)	#3(type B)	#4	#5	#6
chemical analysis	$NbS_{2.9-3.1}$	$NbS_{3.5-4.0}$		$NbS_{2.5-2.8}$	$NbS_{3.4}$	---
x-ray diffraction	$0.5b^*_0$ [a)]	$0.5b^*_0$		$0.5b^*_0$	$0.5b^*_0$	b^*_0
resistive anomaly (T_a) or T_c	------	T_a=140 K	T_a=235 and 140 K	T_c=1.45 K	T_c=1.65 K	T_c=2.15 K
resistivity at 280 K (ohm-cm)	>500	40-50		$1-4x10^{-3}$	$2-6x10^{-3}$	$2x10^{-3}$

a). from ref. 2.

FIGURE CAPTIONS

Fig. 1 Schematic view of distorted and undistorted phases of one-dimensional niobium chain in NbS_3. The main deviation of a distorted structure (type I NbS_3, see ref. 4) from an undistorted structure (ZrS_3 type, see ref. 3) is a displacement of niobium atoms by 4.8 % of b_0 from the midpoint to form Nb-Nb pairs.

Fig. 2 The b-axis x-ray oscillation photographs of the various samples of NbS_3. a) Sulfur-rich NbS_3 (#2 or #3); b) Metallic NbS_3 (#4), T_c=1.45 K; c) Metallic NbS_3 (#5), T_c=1.65 K and d) Metallic NbS_3 (#6), T_c=2.15 K.

Fig. 3 Temperature dependence of the resistivity of nearly stoichiometric NbS_3 and three samples of sulfur-rich NbS_3.

Fig. 4 Temperature dependence of the ac conductivity (a) and its derivative with respect to temperature (b) at several frequencies of sulfur-rich NbS_3. Resistivity anomaly is shown around 140 K.

Fig. 5 Temperature dependence of the ac conductivity (a) and its derivative with respect to temperature (b) at several frequencies of sulfur-rich NbS_3. Two successive resistivity anomalies are shown around 235 and 140 K.

Fig. 6 Temperature dependence of the dc electrical resistance of the metallic NbS_3 (#5) between 4.54 and 0.3 K.

Fig. 7 Resistive transition curves as a function of magnetic field with B$\perp$ a-b plane of the metallic NbS_3 (#5).

Fig. 8 Temperature dependence of the second critical magnetic field ($H_{c2\perp}$) as a function of T/T_c in the B $\perp$ a-b plane configuration in the metallic NbS_3 (#5) (T_c=1.65 K).

Fig. 9 Anisotropy of the critical magnetic field ($H_{c2//}/H_{c2\perp}$) as a function of temperature in the metallic NbS_3 (#5) (T_c=1.65 K).

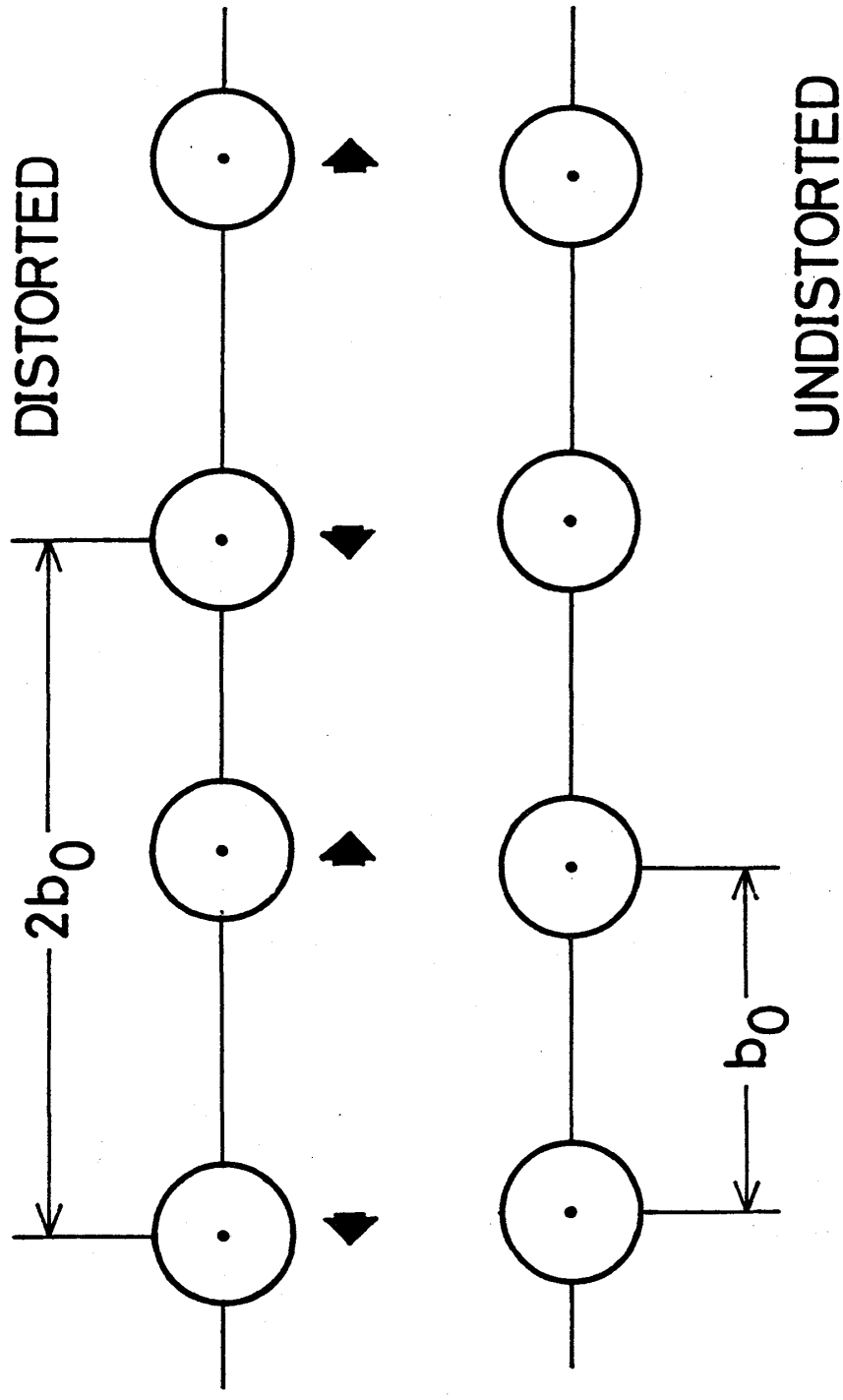

Fig. 1

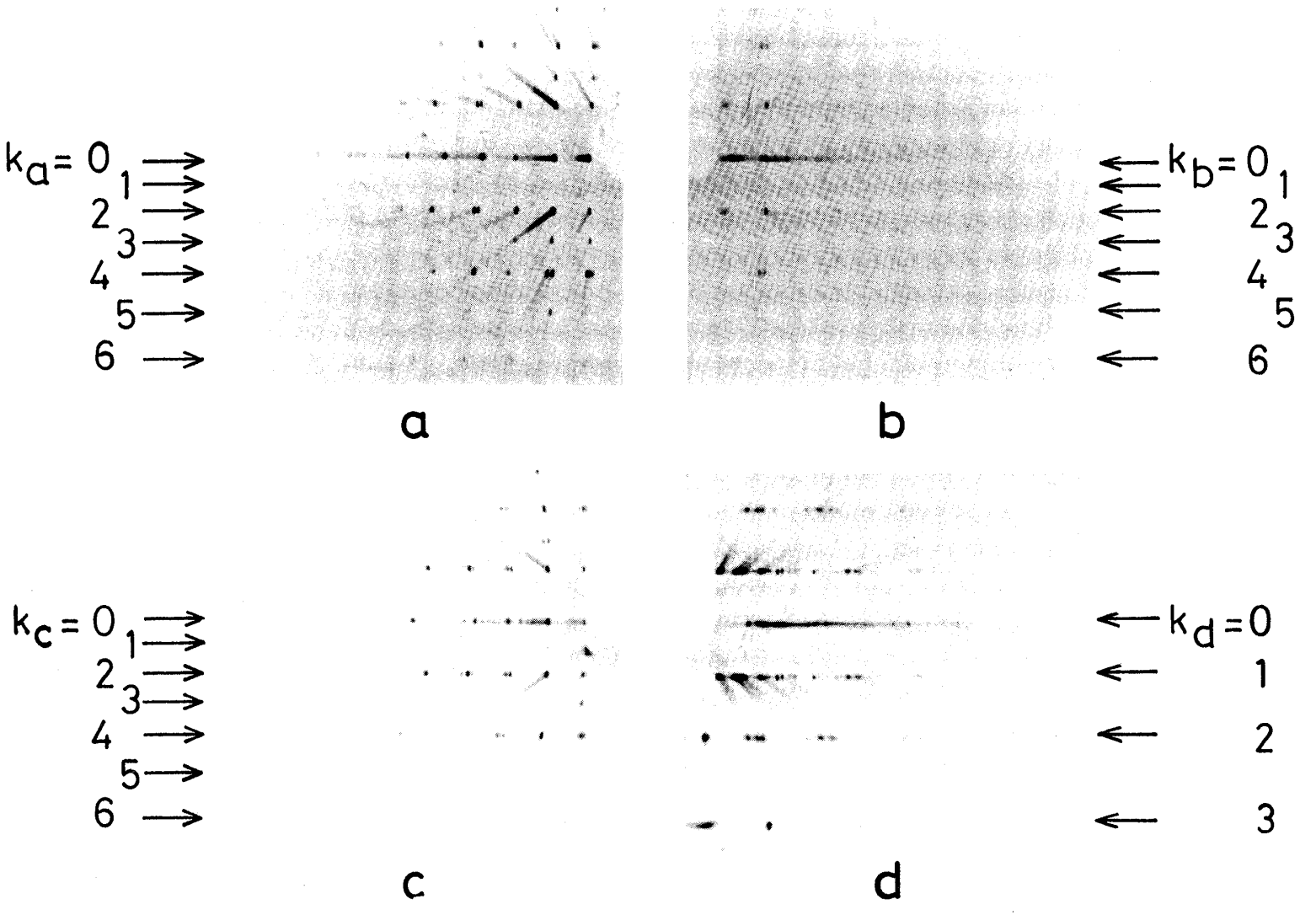
$k_a = 0$ 1 2 3 4 5 6
a
b
$k_b = 0$ 1 2 3 4 5 6
$k_c = 0$ 1 2 3 4 5 6
c
d
$k_d = 0$ 1 2 3

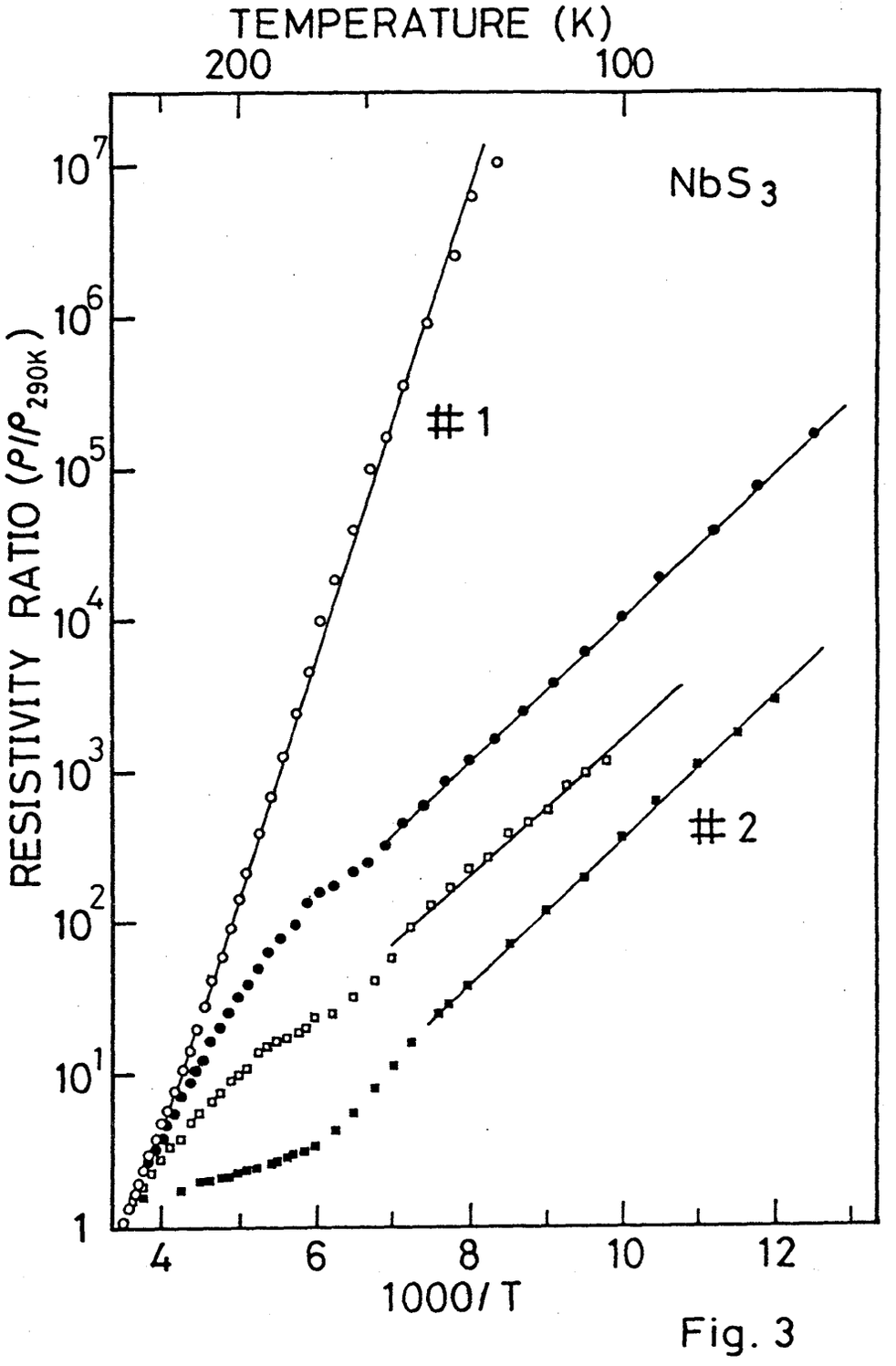
TEMPERATURE (K)
200
100
10^7
10^6
10^5
10^4
10^3
10^2
10^1
1
RESISTIVITY RATIO (ρ/ρ_{290K})
NbS_3
#1
#2
4
6
8
10
12
1000/T

Fig. 3

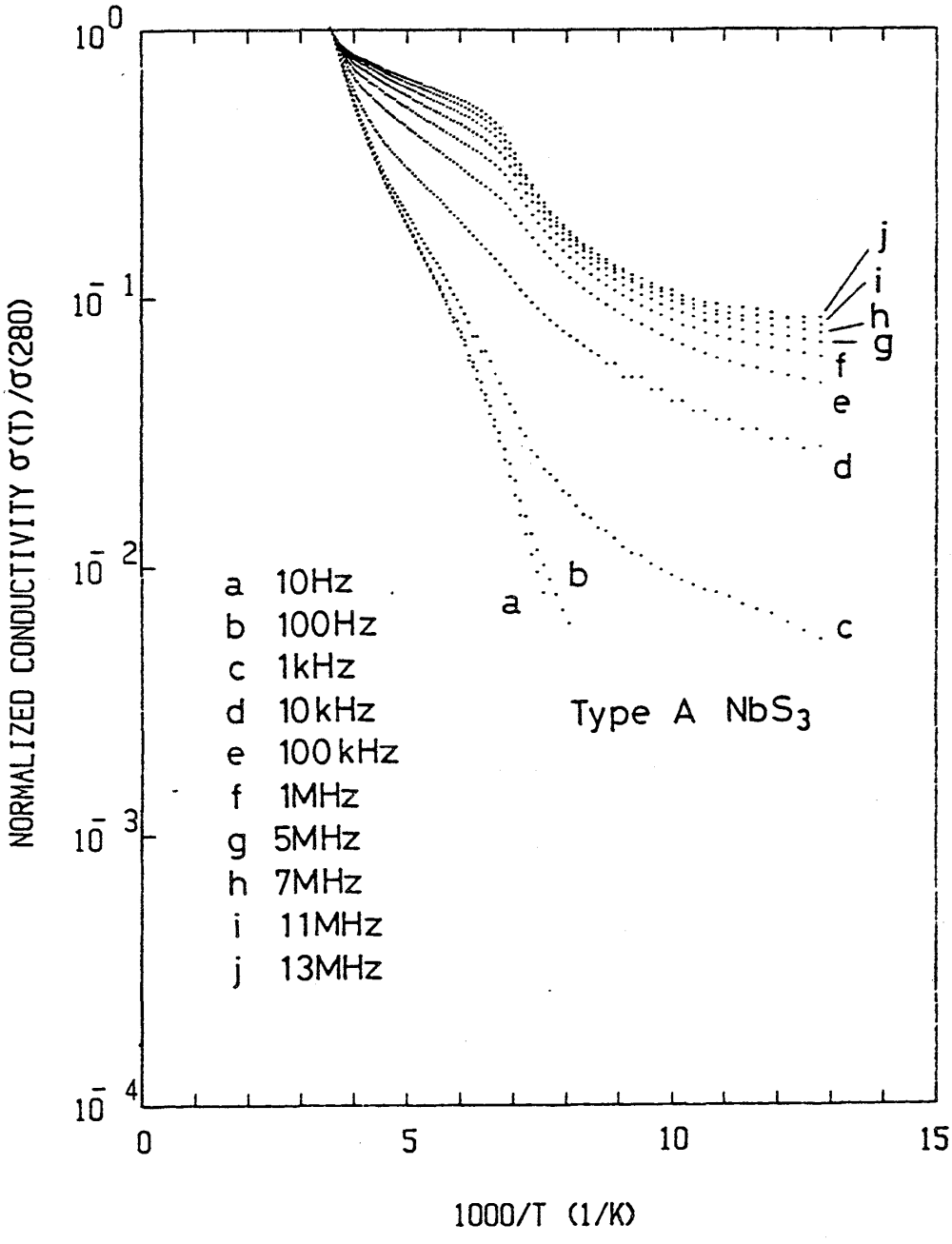
NORMALIZED CONDUCTIVITY σ(T)/σ(280)
1000/T (1/K)
a 10Hz
b 100Hz
c 1kHz
d 10kHz
e 100kHz
f 1MHz
g 5MHz
h 7MHz
i 11MHz
j 13MHz
Type A NbS3

Fig. 4 (a)

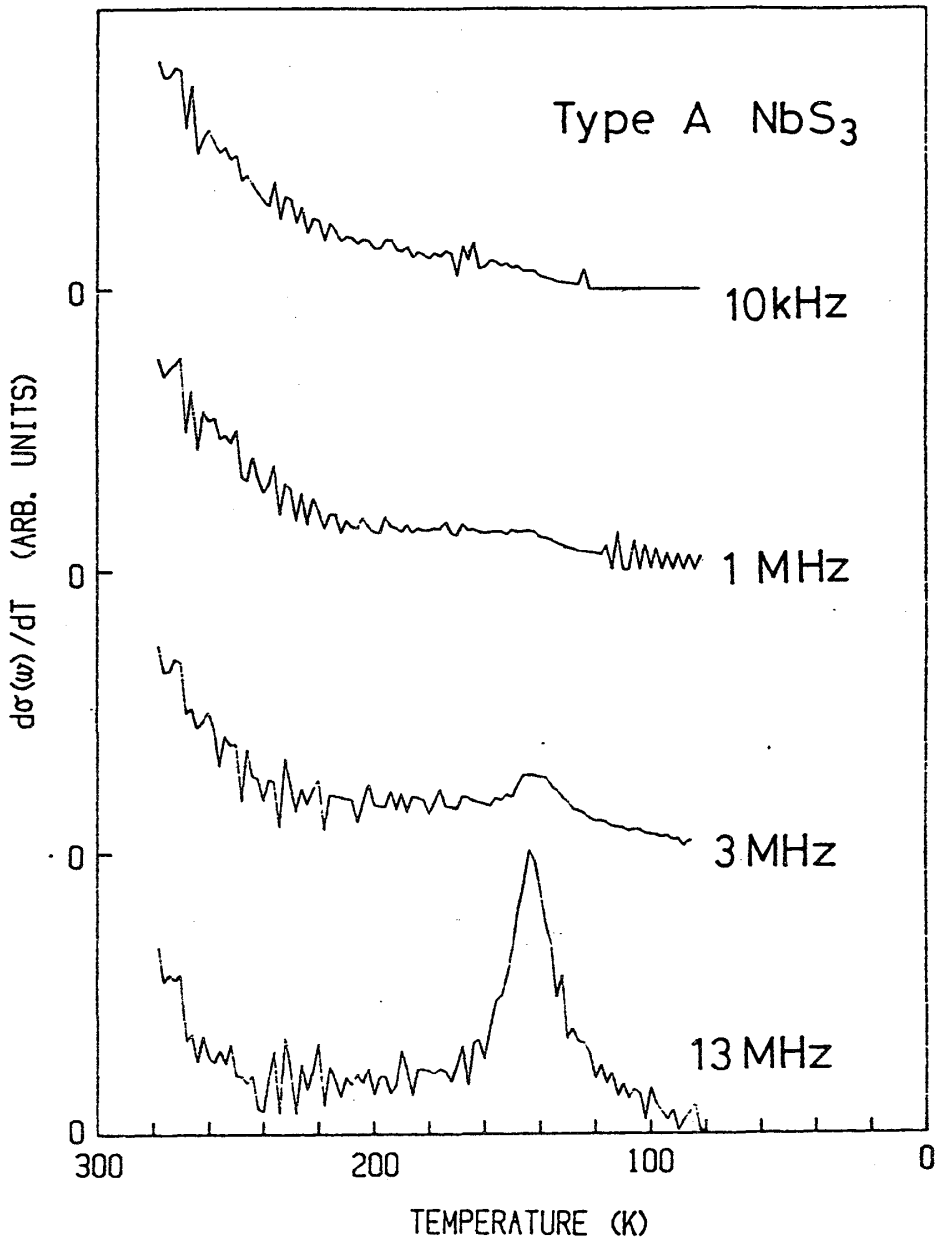
Type A NbS3
10kHz
1 MHz
3 MHz
13 MHz
0
0
0
0
dσ(ω)/dT (ARB. UNITS)
300
200
100
0
TEMPERATURE (K)

Fig. 4 (b)

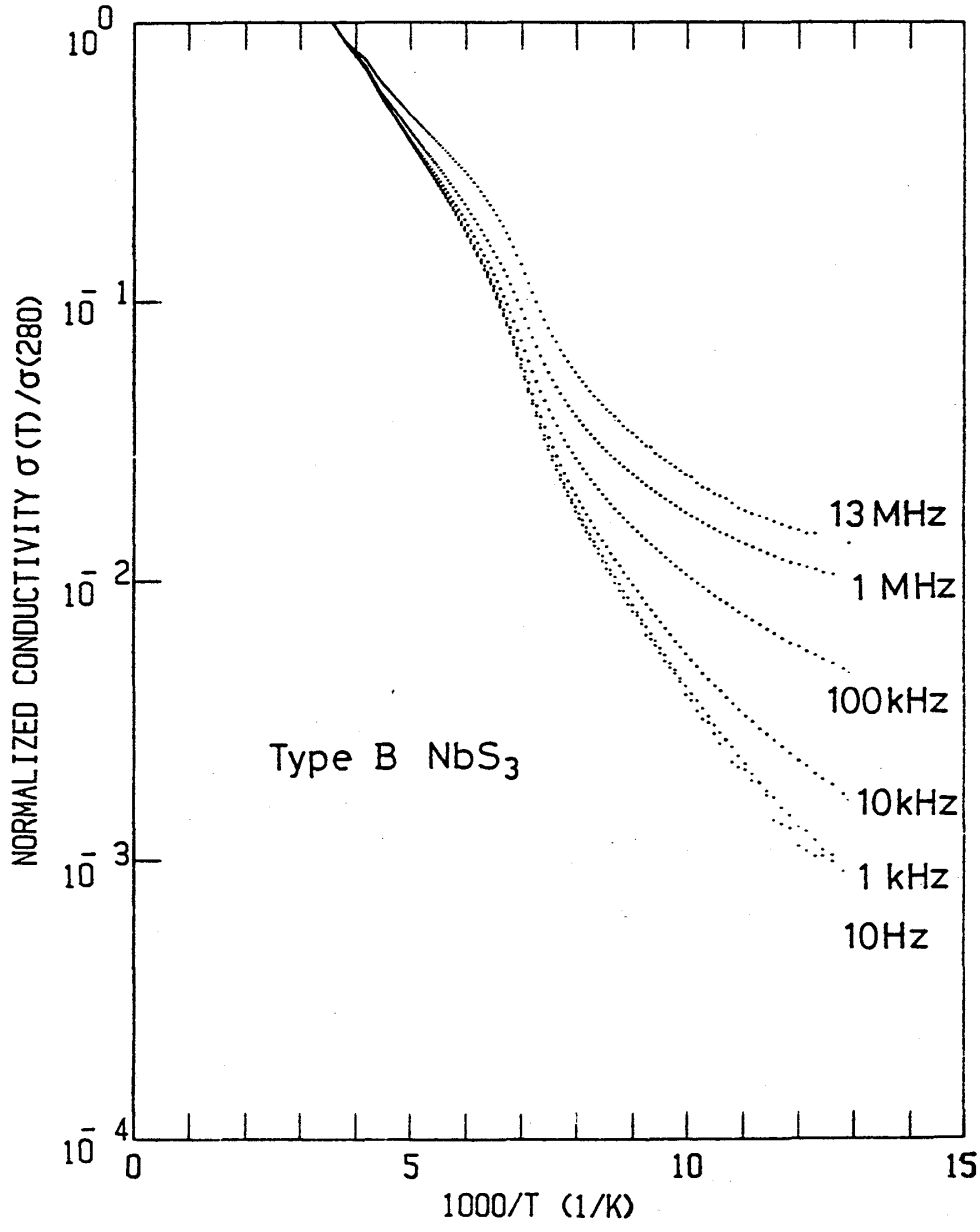
NORMALIZED CONDUCTIVITY σ(T)/σ(280)
10^0
10^-1
10^-2
10^-3
10^-4
0
5
10
15
1000/T (1/K)
13 MHz
1 MHz
100kHz
10kHz
1 kHz
10Hz
Type B NbS3

Fig. 5 (a)

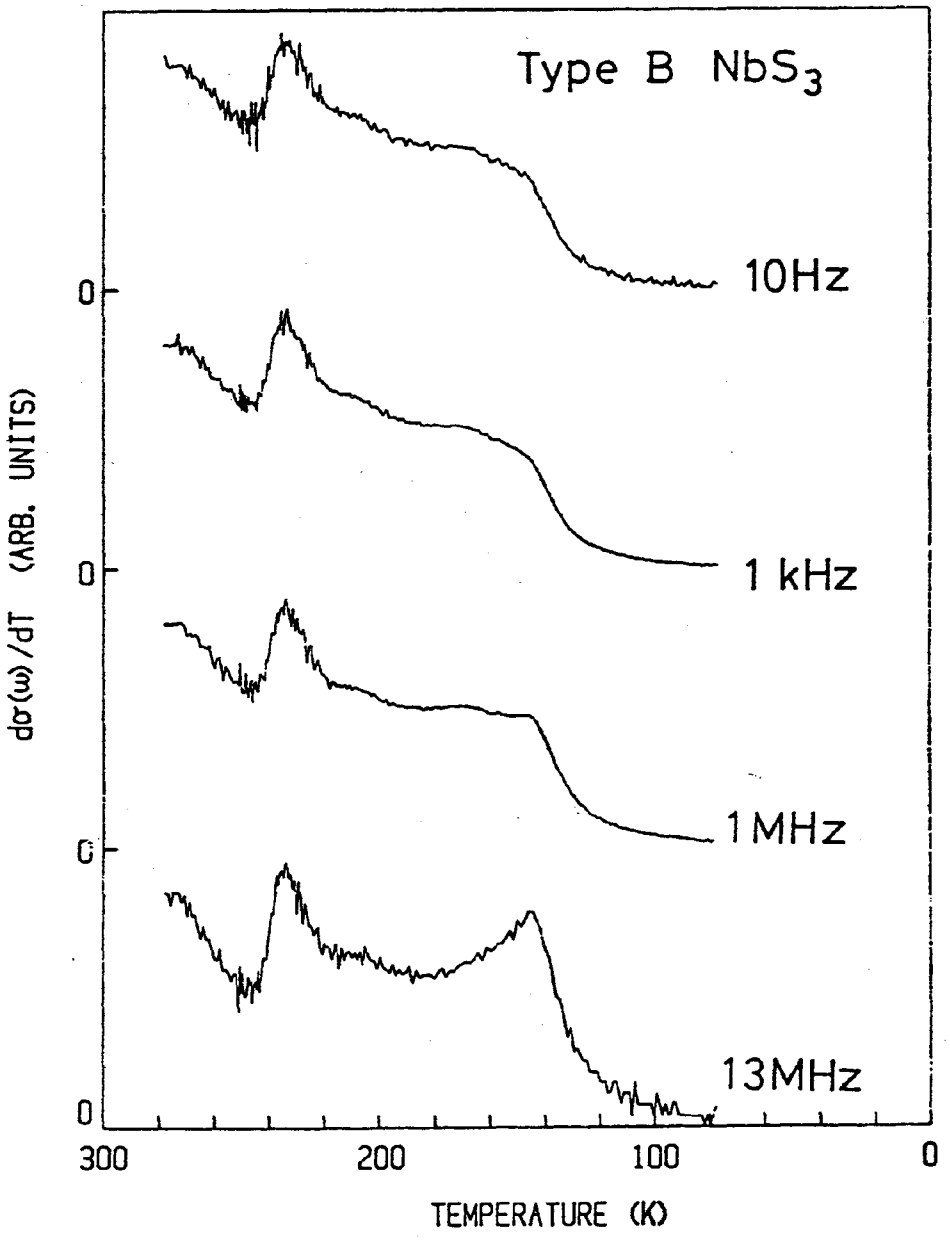
Type B NbS_3
10Hz
1 kHz
1MHz
13MHz
0
0
0
0
300
200
100
0
TEMPERATURE (K)
dσ(ω)/dT (ARB. UNITS)

Fig. 5 (b)

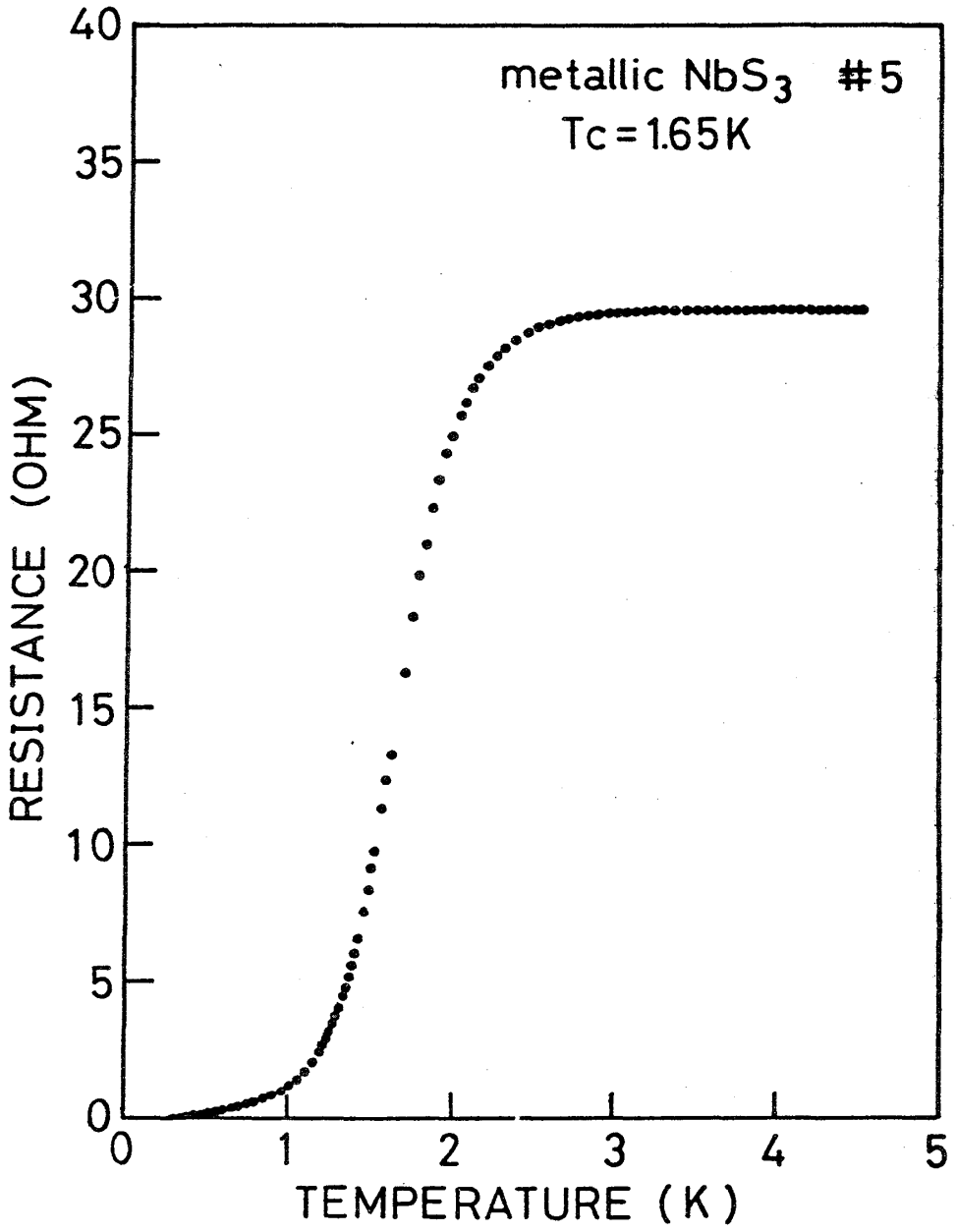
metallic NbS_3 #5
Tc = 1.65K
RESISTANCE (OHM)
TEMPERATURE (K)
0
5
10
15
20
25
30
35
40
0
1
2
3
4
5

Fig. 6

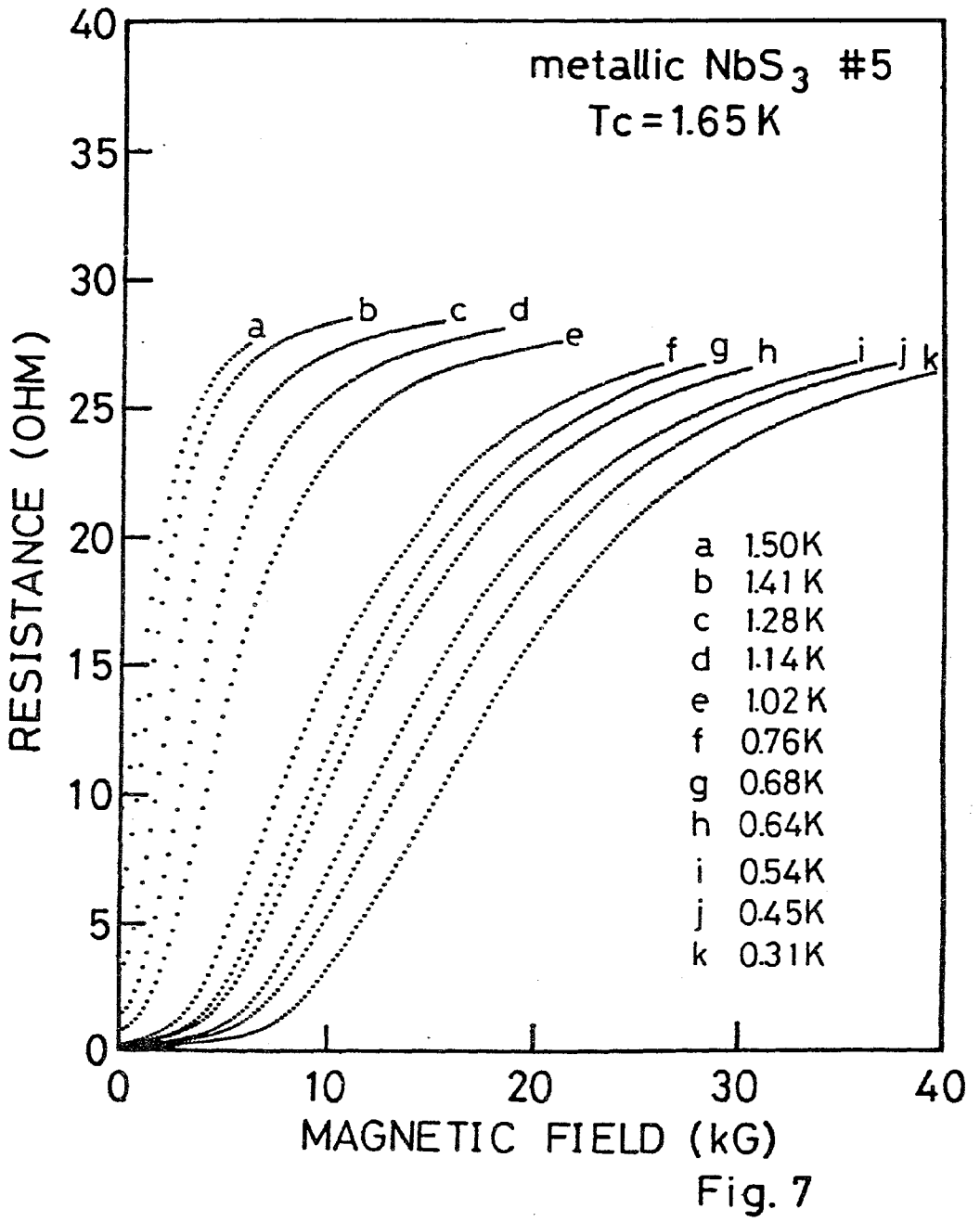
metallic NbS_3 #5
Tc = 1.65 K
RESISTANCE (OHM)
MAGNETIC FIELD (kG)
0
5
10
15
20
25
30
35
40
a 1.50K
b 1.41 K
c 1.28K
d 1.14K
e 1.02K
f 0.76K
g 0.68K
h 0.64K
i 0.54K
j 0.45K
k 0.31K

Fig. 7

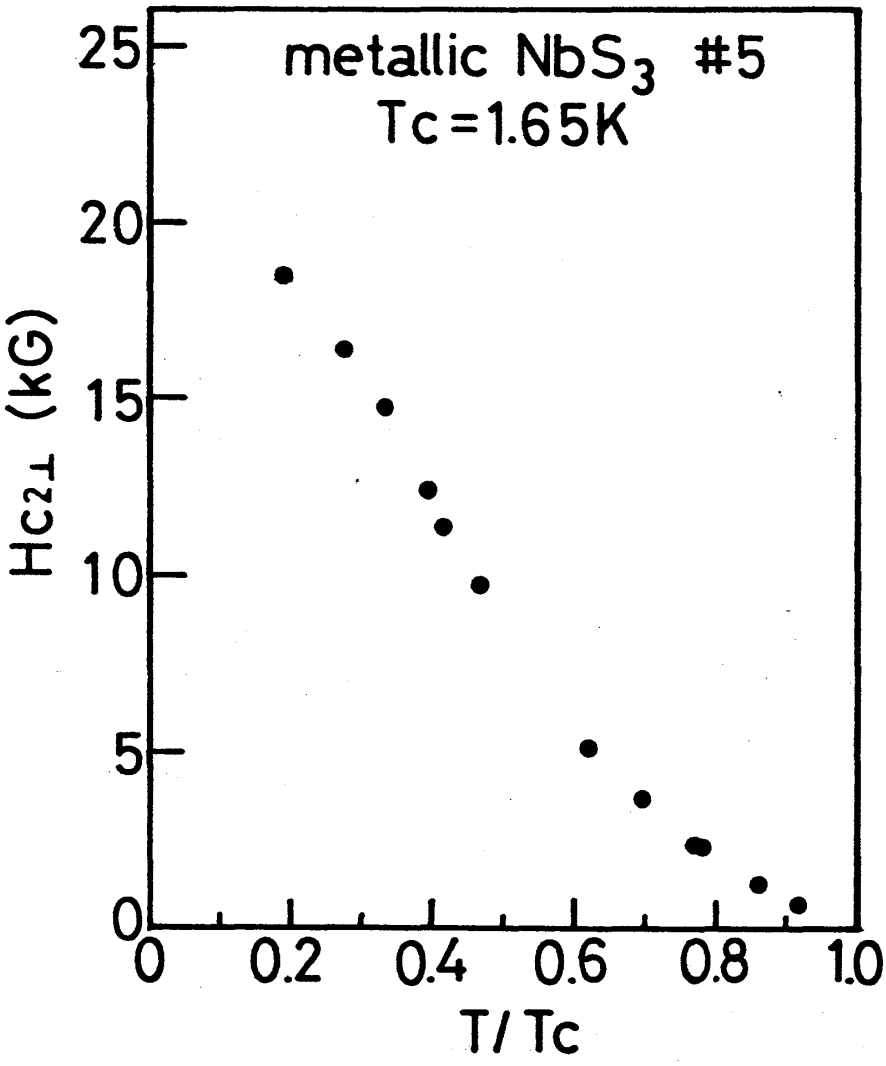
metallic NbS_3 #5
Tc=1.65K
$H_{c2\perp}$ (kG)
25
20
15
10
5
0
0
0.2
0.4
0.6
0.8
1.0
T/Tc

Fig.8

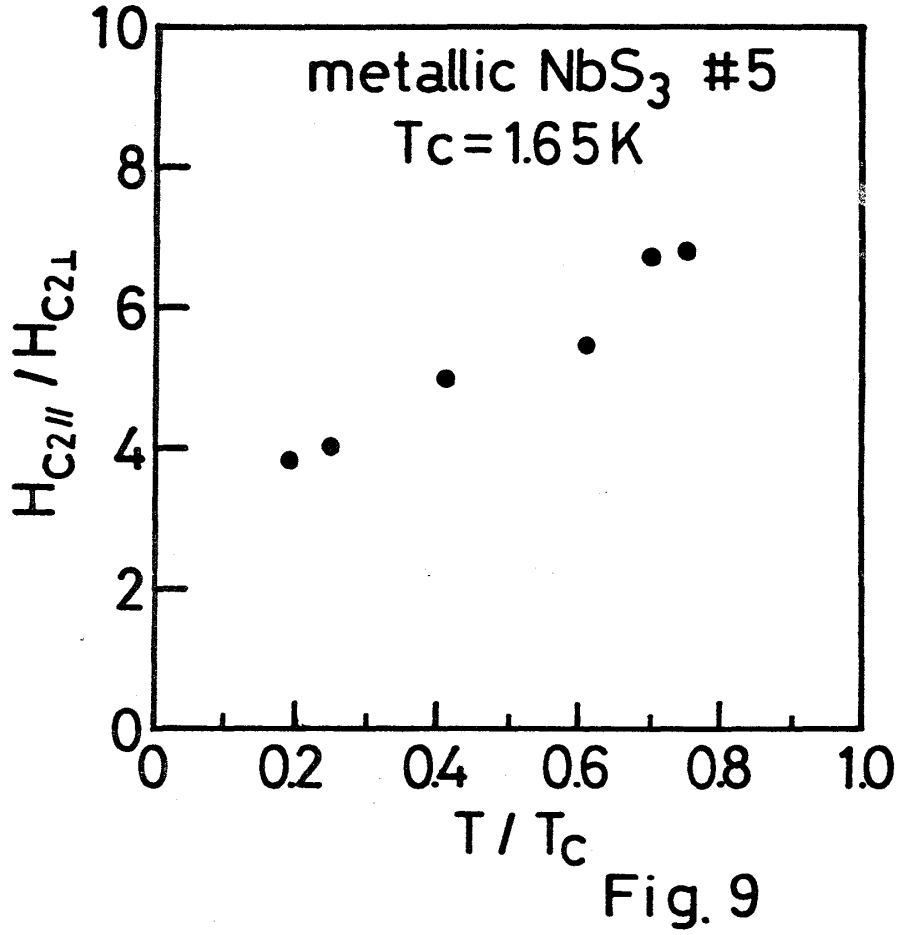
metallic NbS_3 #5
Tc=1.65K
$H_{C2//} / H_{C2\perp}$
T / Tc
0
2
4
6
8
10
0
0.2
0.4
0.6
0.8
1.0

Fig. 9